like *lin-4* and *let-7* mutants, *dcr-1* animals fail to fully switch to adult morphology at the end of larval development, and instead repeat cell divisions and other events characteristic of much younger larvae (*2*). This suggests that Dicer could be required for the production or activity of *lin-4* and *let-7* stRNAs. Indeed, in worms with defective *dcr-1*, the *lin-4* and *let-7* ~22-nucleotide stRNAs are diminished and longer precursor molecules accumulate in their place (*2*). Similarly, when cultured mammalian cells are depleted of Dicer protein, mature *let-7* stRNA is also reduced, and its precursor dsRNA accumulates (*1*). Thus, the double-stranded stem-loop structures of the *lin-4* and *let-7* precursor RNAs seem to be processed by Dicer in worms, flies, and mammals to generate mature ~22-nucleotide stRNAs (see the figure on the previous page).

These new findings reveal that a common maturation cleavage step links the RNAi pathway and developmental gene regulation by stRNAs. Although further work is required to determine which other gene products and processing steps are common to both pathways, it is apparent that some gene products are relatively specialized. For example, whereas Dicer is required for the production of both siRNAs and stRNAs, RDE-4 is specific to RNAi and the production of ~22-nucleotide siRNAs (*15*). In addition, the RDE family proteins ARG-1 and ARG-2 are required for the production of stRNAs, and do not seem to operate in RNAi (*2*).

An emerging hypothesis is that the RNAi and stRNA systems represent different facets of an ancient and widespread strategy for controlling gene expression through small regulatory RNA molecules (*2, 3*). This view is embodied in the notion of a dynamic ribonucleoprotein complex that carries out the steps of the overlapping RNAi and stRNA pathways (*2, 15*). According to this model, the 22-nucleotide siRNA or stRNA binds to the target mRNA to form a base-paired hybrid RNA. The fate of the mRNA depends on the nature of the hybrid: A continuous base-pair hybrid between siRNA and mRNA results in degradation of the mRNA (see the figure). In contrast, an interrupted hybrid in which stRNA binds to the 3′-untranslated region of the mRNA does not result in mRNA degradation but rather prevents it from being translated into protein (*2*).

Among the numerous fascinating issues arising from this work is the degree of interplay between the RNAi and stRNA pathways during normal development. For example, is Dicer activity regulated such that it could influence when and how stRNA-sensitive developmental programs are instigated? Are other genes associated with RNAi also involved in stRNA developmental pathways? Does RNAi directly control mRNA stability during normal development? What other classes of small RNAs are produced by enzymes in the RNAi and stRNA pathways? Undoubtedly, future research into small regulatory RNAs will uncover further layers of complexity. Yet, such work is also likely to reveal the unifying principles that underlie what seems to be an ancient and versatile system for controlling gene expression.

References

1. G. Hutvàgner *et al.*, *Science* **293**, 834 (2001); published online 12 July 2001 (10.1126/science.1062961).
2. A. Grishok *et al.*, *Cell* **106**, 23 (2001).
3. P. A. Sharp, *Genes Dev.* **15**, 485 (2001).
4. R. C. Lee *et al.*, *Cell* **75**, 843 (1993).
5. B. J. Reinhart *et al.*, *Nature* **403**, 901 (2000).
6. A. E. Pasquinelli *et al.*, *Nature* **408**, 86 (2000).
7. P. H. Olsen, V. Ambros, *Dev. Biol.* **216**, 671 (1999).
8. A.J.Hamilton, D.C. Baulcombe, *Science* **286**, 950 (1999).
9. P. D. Zamore *et al.*, *Cell* **101**, 25 (2000).
10. E. Bernstein *et al.*, *Nature* **409**, 363 (2001).
11. S. M. Hammond *et al.*, *Nature* **16**, 293 (2000).
12. S. Parrish *et al.*, *Mol. Cell* **6**, 1077 (2000).
13. S. M. Elbashir *et al.*, *Genes Dev.* **15**, 188 (2001).
14. S. W. Knight, B. L. Bass, *Science*, 2 August 2001 (10.1126/science.1062039).
15. S. Parrish, A. Fire, *RNA*, in press.

PERSPECTIVES: GEOPHYSICS

Deep Diamond Mysteries

Catherine McCammon

Seismological studies indicate that a boundary at 660 km divides the transition zone from the lower mantle, but in the absence of direct samples from this enigmatic region, the nature of the boundary has remained controversial. In particular, the nature of convection—whether it involves the whole mantle or is layered with a boundary at 660 km—remains open. The tantalizing possibility that diamonds may contain tiny inclusions of lower mantle material was recognized in 1984 (*1*). It took another decade for more convincing evidence for such inclusions to be found (*2*). Similar evidence has now been reported from at least 12 localities on five continents (see the first figure). The inclusions provide insights into the 660-km boundary and, more generally, into mantle chemistry, diamond formation, and mantle dynamics.

The mineral ferropericlase accounts for more than half of the inclusions described so far. Other inclusions consist of enstatite and calcium silicate. They are believed to have existed in the perovskite structure at the higher pressures experienced in the lower mantle. To avoid confusion with their upper mantle counterparts, I will refer to these phases as Mg and Ca silicate perovskite, respectively. All three phases could occur elsewhere in the mantle, but their coexistence in individual diamonds (see the second figure) argues strongly for a lower mantle origin because at shallower depths the minerals would combine to produce different phases.

Ni concentrations provide an elegant means of distinguishing lower mantle mineral assemblages from those originating at shallower depths (*3*). Experiments show that Ni is incorporated preferentially into ferropericlase at high pressures, leaving Mg silicate perovskite depleted (*4*). Upper mantle enstatite normally contains 0.1 to 0.2% Ni by weight, but the enstatite (formerly Mg silicate perovskite) found in lower mantle inclusions contains less than 0.02% Ni (*4*). Rare earth elements are concentrated in Ca silicate perovskite lower mantle inclusions relative to ferropericlase and Mg silicate perovskite, which agrees with experimental work for lower mantle assemblages.

Phases identified in lower mantle assemblages also include quartz (likely converted from the high-pressure mineral stishovite) and the enigmatic tetragonal almandine pyrope phase (TAPP) (*5*). Although chemically similar to garnet, TAPP has a relatively open crystal structure and may have crystallized during the ascent of the host diamond (*6*).

We cannot determine the pressure and temperature conditions of the formation of the inclusions, but the composition of Mg silicate perovskite provides a means to estimate the depth of their origin (*2, 3*). Mantle Al is concentrated in garnet, which persists to depths greater than 660 km. However, with increasing pressure, garnet eventually transforms to the perovskite structure and hence the concentration of Al in Mg silicate perovskite increases. Nearly all Mg silicate perovskite inclusions have low Al concentrations, which could occur only at the top of the lower mantle where garnet is also present. A small number of inclusions, however, suggest a much deeper origin. One Mg silicate perovskite grain was found to contain

The author is at the Bayerisches Geoinstitut, Universität Bayreuth, D-95440 Bayreuth, Germany. E-mail: catherine.mccammon@uni-bayreuth.de

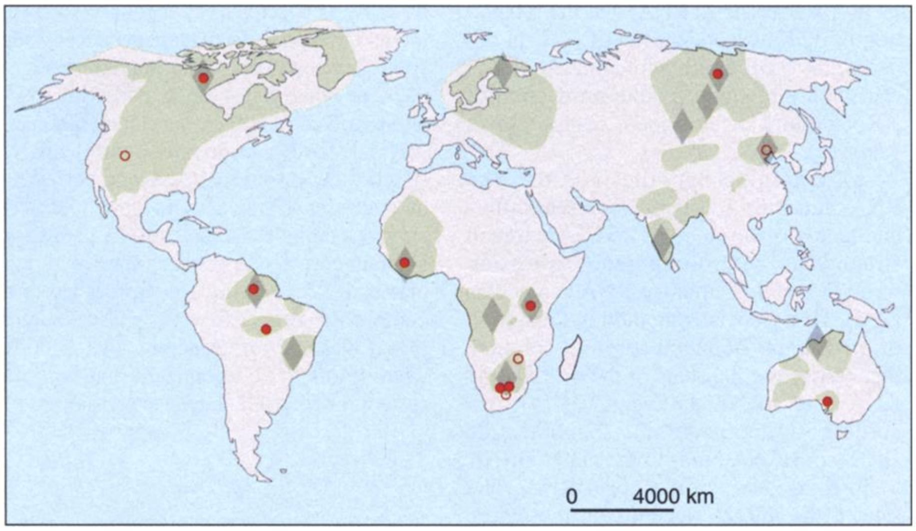

Distribution of lower mantle inclusions. Superdeep diamonds from most locations contain multiple inclusions that provide convincing proof of lower mantle origin (solid red circles), although some are still open to question (open red circles). Also shown are the global distribution of cratons (yellow shading; older than 1600 million years), which are the relatively stable interiors of continental plates, and major diamond deposits (gray diamonds). [Adapted from (*15*)]

more than five times the usual concentration of Al (*2*). The occurrence of extremely iron-rich ferropericlase in one inclusion was interpreted (*2*) to indicate an origin near the core-mantle boundary.

The phase assemblages in the inclusions reflect primarily the conditions during diamond crystallization, but the original source rock material may leave some geochemical signature. Ca silicate perovskite inclusions are enriched in trace elements many times above primitive mantle levels, suggesting an enriched source such as subducted crust (*2*, *4*, *7*). A crustal source is also supported by the observation of positive Eu anomalies in Ca Silicate perovskite (*2*, *4*). The best known cause of such anomalies is associated with the crystallization of feldspar, which implies crustal origin because feldspar only crystallizes at low pressures. However, not all Ca silicate perovskite inclusions exhibit such anomalies (*8*). A subducted crustal source is also supported by data from (*9*), where lower mantle inclusions are associated with upper mantle diamonds containing subducted minerals. Other less likely possibilities can account for the trace element patterns, but the general consensus seems to be that the source rock for most lower mantle inclusions is subducted oceanic crust.

The diamonds that surround the lower mantle inclusions tell a different story. Carbon isotopic compositions resemble those of the primitive mantle (*2*, *8–10*), in contrast to upper mantle diamonds, which show much lower and more scattered values. The carbon in lower mantle diamonds therefore does not originate from subducted material. Lower mantle inclusions show evidence of both oxidizing (*2*) and reducing (*2*, *8*, *9*) conditions. Diamond precipitation (*2*, *11*) may therefore be a fortuitous by-product of the complex redox conditions at the top of the lower mantle (*12*, *13*).

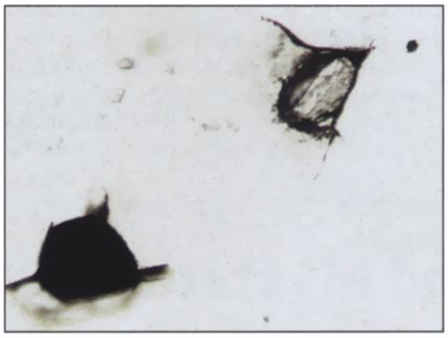

A piece of the lower mantle. In this diamond, ferropericlase (black) coexists with enstatite (transparent), providing evidence of lower mantle origin because these minerals would recombine to make olivine at shallower depths. Fractures likely arose during the transformation of Mg silicate perovskite to enstatite as pressure decreased during ascent. The long axis of the transparent crystal is about 150 μm long.

Nearly all lower mantle diamonds are classified as Type II, meaning that nitrogen concentrations are very low. In contrast, 98% of upper mantle diamonds are Type I. The low concentration of nitrogen contradicts geochemical models that describe the lower mantle as a nitrogen reservoir and may indicate that nitrogen is mostly excluded during diamond crystallization or has been lost to the core during accretion (*10*). The small amounts of nitrogen in lower mantle diamonds show a high degree of clustering, which only occurs during long mantle residence times and/or temperatures higher than are typical for diamond crystallization (*8–10*). Furthermore, most lower mantle diamonds show a high degree of plastic deformation and complex growth and etching features (*3*, *9*, *10*). The diamonds apparently had a tortuous route to the surface.

The many unique characteristics of lower mantle diamonds and their inclusions provide convincing evidence that they did indeed originate in the lower mantle and fuel the long-running debate over whether mantle convection is layered or not. The narrow distribution of carbon isotope values across global sources suggests that the lower mantle has a homogeneous carbon isotopic composition, which argues against extensive mixing of the upper and lower mantle. Trace element enrichment argues for a subducted source, thereby supporting the idea that descending slabs pile up at the 660-km discontinuity (*14*). This presents a picture of layered convection where limited mixing occurs at the 660-km boundary (*2*), but also argues for the presence of mantle plumes that extend below 660 km to deliver diamonds into our hands.

Lower mantle inclusions therefore favor a hybrid model of mantle convection, where limited mixing occurs but chemical inhomogeneities between the upper and lower mantle are preserved. Many uncertainties remain, but at least one dispute has been settled—the very existence of lower mantle diamonds provides perhaps the strongest evidence yet that the 660-km boundary is not impenetrable.

References

1. B. H. Scott-Smith *et al.*, in *Kimberlites and Related Rocks*, J. Kornprobst, Ed. (Elsevier, Amsterdam, 1984), pp. 121–142.
2. B. Harte *et al.*, in *Mantle Petrology: Field Observations and High-Pressure Experimentation: A Tribute to Francis R. (Joe) Boyd*, Y. Fei *et al.*, Eds. (Geochemical Society, St. Louis, MO, 1999), vol. 6, pp. 125–153.
3. T. Stachel *et al.*, *Contrib. Mineral. Petrol.* **140**, 16 (2000).
4. S. E. Kesson, J. D. Fitz Gerald, *Earth Planet. Sci. Lett.* **111**, 229 (1991).
5. J. W. Harris *et al.*, *Nature* **387**, 486 (1997).
6. L. W. Finger, P. G. Conrad, *Am. Mineral.* **85**, 1804 (2000).
7. W. Joswig *et al.*, *Earth Planet. Sci. Lett.* **173**, 1 (1999).
8. F. V. Kaminsky *et al.*, *Contrib. Mineral. Petrol.* **140**, 734 (2001).
9. R. Davies *et al.*, in *The J.B. Dawson Volume, Proceedings of the VII International Kimberlite Conference*, J. J. Gurney *et al.*, Eds. (Red Roof Design, Cape Town, South Africa, 1999), vol. 1, pp. 148–155.
10. M. T. Hutchison *et al.*, in *The J.B. Dawson Volume, Proceedings of the VII International Kimberlite Conference*, J. J. Gurney *et al.*, Eds. (Red Roof Design, Cape Town, South Africa, 1999), vol. 1, pp. 372–382.
11. P. Deines, *Geochim. Cosmochim. Acta* **44**, 943 (1980).
12. C. A. McCammon, *Nature* **387**, 694 (1997).
13. C. A. McCammon *et al.*, *Science* **278**, 434 (1997).
14. A. E. Ringwood, *Geochim. Cosmochim. Acta* **55**, 2083 (1991).
15. S. E. Haggerty, *Science* **285**, 851 (1999).

CREDIT: (TOP) ADAPTED FROM (15)